

Strong isotope effects in the $F + HD$ reactions at the low-energy interval: a quantum-mechanical study

Michael Baer^{*,1}

Academia Sinica, Institute of Atomic and Molecular Sciences, Taipei 10764, Taiwan, ROC

Received 22 July 1999; in final form 9 August 1999

Abstract

This Letter reports on a quantum-mechanical coupled-state study of the reactions $F + HD \rightarrow FH + D$ and $F + DH \rightarrow FD + H$ at four (low) energies namely 21, 35, 51 and 61 meV. Vibrational state-to-state integral and differential cross-sections are presented. The main results are: (a) the FD products are always distributed backward; (b) the FH products show forward–backward distributions at the two higher energies, a tri-peak distribution at the third energy and a backward distribution at the lowest energy; (c) the calculated integral cross-sections yield a strong isotope effect where the FH product is favored over the FD product. © 1999 Elsevier Science B.V. All rights reserved.

1. Introduction

The $F + XY$ ($X, Y = H, D$) systems have played an important role in the study of elementary chemical reactions for the last three decades [1]. The number of studies devoted to this reaction probably exceeds the number of studies relating to any single system in chemical physics. Still, this system possesses unrevealed features that justify additional studies. It all started with the crossed molecular beam experiments by the Lee group, which provided the first vibrational resolved differential cross-sections for all four isotopic systems [2–4], and with the low pressure arrested relaxation chemiluminescence experiments of the Polanyi group [5–7], that yielded,

for these systems, the first products vib-rotational distributions. More recently it was the Toennies group [8–11] that succeeded in obtaining the first vib-rotational resolved differential cross-sections for $F + D_2$. These experiments together with a simultaneous quantum-mechanical treatment established the existence of rotational bi-modal distributions formed in this reaction [10,11]. Some time later, two other groups, independently, explored the rotational distributions of HF products using IR-based techniques. In one experiment, Dharmasena et al. [12] measured the relative population of several rotational states belonging to $v' = 1, 2$ and in another, Chapman et al. [13] measured, as a function of energy, state-to-state vib-rotational integral cross-sections. A few months ago the Toennies group [14] completed an additional series of experiments in which for the first time the vib-rotational state resolved differential cross-sections for $F + H_2$ were measured. More experiments

^{*} Permanent address: Soreq NRC, Yavne 81800, Israel. Fax: +972-8-9456017; e-mail: mmbaer@netvision.net.il

¹ Guest Professor at the Academia Sinica, IAMS.

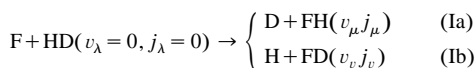
are currently being performed by Liu [15] at the IAMS in Taipei, with the aim of measuring state-to-state integral and differential cross-sections at low energy for the F + HD system.

The quantum-mechanical (QM) study of these systems started in 1973 with the publications by Wu et al. [16] and by Schatz et al. [17]. These studies were followed by many others, among them the first attempt to simulate Lee's experiments which was done by Jellinek et al. [18] employing the three-dimensional reactive infinite order sudden approximation (RIOSAs) [19]. This attempt, compared to present achievements, can be considered to be somewhat 'naive'. This could be due to the approximations involved in the RIOSAs but it is more likely attributable to the shortcomings of the M-5 potential energy surface (PES) [20] employed in these calculations. Indeed, a few years later Takayanagi et al. [21] employed the same RIOSAs but with a more successful PES, namely a modified London–Polanyi–Eyring–Sato surface with a non-linear saddle point (this PES has numerous features in common with the recent advanced Stark–Werner PES [22]) and got much more relevant results for these reactions although still far from the present achievements. It was only after Stark and Werner (SW) made available their PES [22] that theory and experiment started to converge. In almost all subsequent QM calculations [10,11,23–25] a consistent reasonably good fit between the above scattering experiments and theory was achieved. In this respect it is important to mention also a very good fit achieved, employing the SW PES, in a different type of calculations, namely that of rate-constants. Here the success of the QM treatment [26,27] in producing correctly the experimental results for a whole range of temperatures for the two isotopic reactions $F + X_2$ ($X = H, D$), and in particular for their isotopic ratio [26] that was measured directly and independently [28,29], which increased the confidence in both the SW PES and the QM approaches.

A few years ago Rosenman et al. [26] revealed a unique feature of the SW PES, namely the existence of a dynamic QM potential barrier of height ~ 0.75 kcal/mol that is thin enough to permit the hydrogen atoms to penetrate through it almost freely but yet broad enough to significantly reduce the penetration capability of the deuterium atoms. This selective

ability was already noticed while calculating the cross-sections of the two isotopic reactions $F + X_2$ ($X = H, D$). Whereas for hydrogen the threshold (in the case of $j = 0$) was practically zero, it was ~ 0.5 kcal/mol for deuterium.

In this Letter we report on QM integral and differential cross-sections for the three-arrangement reactions:



as calculated in the low-energy range $21 \text{ meV} \leq E_{tr} \leq 61 \text{ meV}$. Castillo and Manolopoulos (CM) [23] considered these reactions and calculated integral and differential cross-sections at the two 'experimental', energies, namely $E_{tr} = 1.35$ and 1.84 kcal/mol. They revealed the existence of a strong isotopic effect in the angular distributions for the two products but only a slight one for the integral cross-sections. In this Letter we shall show that, in the low-energy region, isotope effects also appear in integral cross-sections.

2. Theoretical comments

The approach, developed by the present author together with his colleagues, was described in detail on several occasions and there is no necessity to go into too much detail once again [30–34]. However, since this is the first time that a three different-arrangement-channels (AC) system is treated (namely, (F, HD), (FH, D) and (FD, H)), it could be of importance to remind the reader of some details and show how efficient and friendly this method is, even in such a complicated case like this one.

The aim of the calculation is to obtain the following matrix element:

$$S(t_\alpha | t_{0\lambda}) = \left\{ \delta_{t_{0\lambda} t_\alpha} \delta_{\alpha\lambda} + \frac{m}{i\hbar^2} \langle \psi_{t_\alpha} | V_{t_\alpha} | \psi_{t_{0\lambda}} + \chi_{t_{0\lambda}} \rangle \right\} \times \exp(i\varphi_{t_\alpha}). \quad (1)$$

Here the function: $\Psi_{t_{0\lambda}} = \psi_{t_{0\lambda}} + \chi_{t_{0\lambda}}$ is the total wavefunction defined in the λ AC (including an extended interaction region), $\psi_{t_{0\lambda}}$ is the unperturbed part of the total wavefunction which contains the correct boundary conditions, and $\chi_{t_{0\lambda}}$ is the per-

turbed part which is a solution of the following inhomogeneous Schrödinger equation:

$$(E - H) \chi_{t_{0\lambda}} = V_{t_{0\lambda}} \psi_{t_{0\lambda}}. \quad (2)$$

The potential $V_{t_{0\lambda}}$ in Eqs. (1) and (2), is the perturbed potential in the α -AC, $t_{0\lambda}$ stands for a set of quantum numbers related to the α -AC, i.e. $(v_{\alpha}, j_{\alpha}, \Omega_{\alpha}, J)$, $\varphi_{t_{0\lambda}}$ is the $t_{0\lambda}$ th (elastic) phase shift and the δ 's are the ordinary Kronecker delta functions. In all cases λ labels the initial AC and α any of them, namely, either the initial one (and then $\alpha \equiv \lambda$) or one of the exchange (reactive) ACs. As for the four quantum numbers: v and j are the vibrational and rotational quantum numbers, respectively, J is the total angular momentum quantum number and Ω is the projection of J and j along the respective translational vector R . It is important to emphasize that $t_{0\lambda}$ stands for the initial set of quantum numbers. The main advantage of this approach is that once Eq. (2) is solved (and this can be done only with the help of negative imaginary potentials – NIPs [35]) then all required S -matrix elements follow from a straightforward integration over the λ -AC (the initial AC) coordinates as given in Eq. (1). The solution of Eq. (1) is carried out employing the ordinary reagents Jacoby coordinates. In what follows the incoming λ -AC is the F + HD AC, the reactive μ -AC is the FH + DAC and the reactive ν -AC is the FD + HAC. The results reported here were obtained by employing the coupled-states approximation (CSA) [36].

As was mentioned above the calculation of each state-to-state S -matrix element is done separately. A check for the approach is to calculate, for a given J , the reactive probability for each of the two products, namely, $P_{\mu}(J)$ for FH and $P_{\nu}(J)$ for FD, and compare their sum ($P_{\mu}(J) + P_{\nu}(J)$) with the total reactive probability, $P_T(J)$, as obtained (independently) from the corresponding non-reactive S -matrix elements. It turns out that for all reported energies and for most J -values, indeed, the relation:

$$P_{\mu}(J) + P_{\nu}(J) \approx P_T(J) \quad (3)$$

is approximately maintained. However, we also found that at some J values $P_{\mu}(J)$ is too large (this happens for the J values that are directly associated with the resonance, as will be discussed later). Therefore the J -dependent, state-to-state S -matrix elements were normalized accordingly. Thus if

$S(t_{\mu}, J)$ is the original S -matrix element for the μ -AC, then the modified one, $S_m(t_{\mu}, J)$, is given in the form:

$$S_m(t_{\mu}, J) = \sqrt{\frac{P_T(J) - P_{\nu}(J)}{P_{\mu}(J)}} S(t_{\mu}, J). \quad (4)$$

This requirement for normalization was somewhat surprising for us because, so far, we had never had to carry it out. Even in the present case, while considering the total probability functions, $P_T(J)$, no normalization was needed. Thus it could very well be that the CSA becomes sensitive in case the reaction, for a given J at a given arrangement channel, is dominated by a strong resonance.

As a final subject we would like to refer to the type of NIPs employed in our calculations. Since the energy of the reagents (and of course of the non-reactive products) is very low we are forced to employ soft and long-range NIPs in this AC. Indeed, we chose the Neuhauser–Baer linear NIPs with a range of 2 Å and a height of 0.07 eV to ensure full absorption and no reflection. This large increase in the total length of the entrance AC hardly affects the numerical effort.

3. Computational results

In the present study we concentrate on the (very) low-energy region, namely the energy range 21 meV $\leq E_{tr} \leq$ 61 meV. Two types of results will be discussed.

3.1. Vibrational state-to-state differential cross-sections

Here we show results for two energies. In Fig. 1 the differential cross-sections for $E_{tr} = 61$ meV as calculated for the two reactive ACs in Eq. (1) are shown. The results in this figure are not novel: a calculation, by CM [24], employing an ‘exact’ treatment yielded results which in general look like ours. However, a more detailed inspection reveals some quantitative differences. In the case of FH the two treatments yield angular distributions with strong backward and forward maxima but the CM distribu-

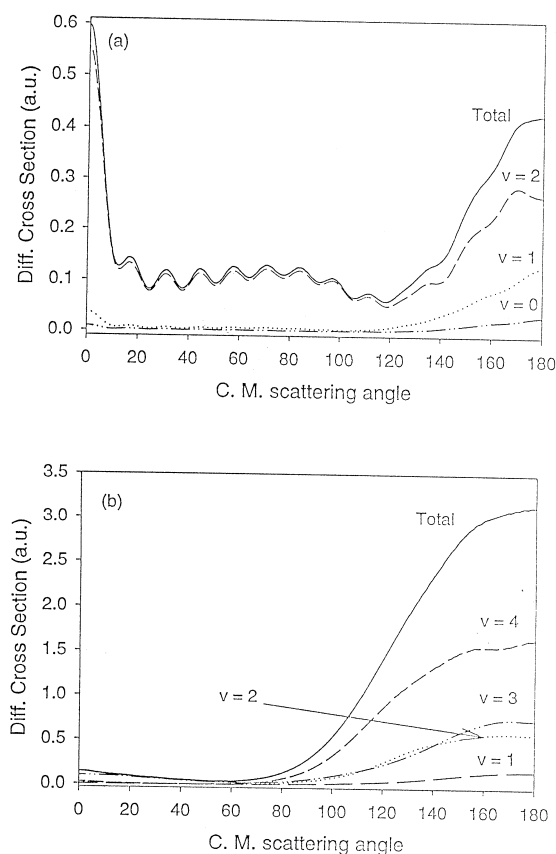


Fig. 1. Vibrational state-to-state differential cross-sections for the F+HD reactions as calculated at $E_{tr} = 61$ meV: (a) results for $F+HD \rightarrow FH+D$ and (b) results for $F+DH \rightarrow FD+H$.

tion is milder. For instance, the ratio between cross-sections belonging to a central angle vs. cross-sections at 180° or 0° is about 1:3 in the CM case and about 1:4 in our case. As for FD the two treatments yield strong backward distributions but in this case it is the present angular distribution that is milder: for instance, the ratio $\sigma(120^\circ)/\sigma(180^\circ)$ is about 1:3 in the CM case and only about 1:2 in our case. Although these differences may be regarded by some as significant we think that the CSA, as incorporated in our approach, is capable of yielding reasonable state-to-state differential cross-sections and therefore is trustworthy (even those for FH for which some of the S -matrix elements had to be renormalized). In this respect it is worthwhile to mention that our

opacity functions are also similar to those of CM, except for the sharp peak at $J = 3$ (designated by them as B). Our calculations do not support the existence of this abrupt behavior.

We also calculated differential cross-sections for $E_{tr} = 51$ meV (not shown here) and got similar distributions as for $E_{tr} = 61$ meV.

In Fig. 2 are presented the differential cross-sections for a lower energy, namely $E_{tr} = 35$ meV. It is well noticed that whereas the FD channel yields a 'normal' backward distribution, similar to what was encountered at the previous case, the FH channel produces a different distribution, which is to a certain extent novel. It is well noticed that in addition to the strong forward and backward maxima which are

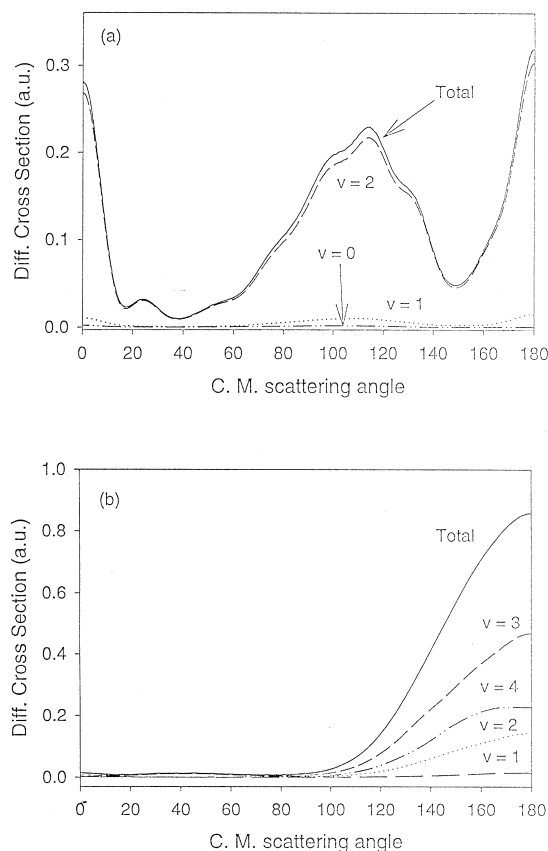


Fig. 2. Vibrational state-to-state differential cross-sections for the F+HD reactions as calculated at $E_{tr} = 35$ meV: (a) results for $F+HD \rightarrow FH+D$ and (b) results for $F+DH \rightarrow FD+H$.

typical for the low-energy FH channel (in the case of $F + H_2$ as well as in the case of $F + HD$) here a new feature is encountered. Around the center-of-mass angle $\theta \approx 110^\circ$ the angular distribution reaches a third maximum that is only rarely seen in scattering calculations. In fact, we encountered such a (third) peak in the $Li + HF$ reaction for low (translational) energies [34]. The $Li + HF$ result can be attributed to the fact that the product molecule, LiF , emerges from the interaction mainly with an $\Omega = J$ value. In such a case it is well known that the Legendre polynomials $P_\Omega^J(\theta)$ attain their maximum at $\theta = \pi/2$, and therefore it is expected for the angular distribution to peak at this angle. Here we found that the FH molecule emerges from the interaction region mainly with $\Omega = \Omega_\mu = 0$ and therefore the situation is more complicated. Since we cannot attribute this phenomenon to any obvious cause a possible explanation is as follows. Due to the strong tunneling processes on one hand and the existence of shallow potential wells on the other this low-energy region is vulnerable to interference effects that for different energies may lead to different patterns for the differential cross-sections. Indeed, we found that the shapes of the differential cross-sections are very sensitive with respect to the energy. In this respect it is important to mention that we also calculated differential cross-sections for $E_{tr} = 21$ meV (not shown here) and obtained an unexpected pure backward distribution.

As for the comparison with experiment there exist the well-known results of the Lee group which were obtained at two energies, one of which is $E_{tr} = 60$ meV. It is difficult for us to compare the present differential cross-sections with the Lee differential cross-sections as these were never transformed to the center-of-mass system and we lack the means to transform ours to the laboratory system. However, CM [24] did a careful analysis in this respect, and we cannot add much to it except for one comment. Comparing our angular distributions to theirs it is seen that the present curve has a more pronounced peak in the forward direction. If all that is missing (as was claimed by CM) in order to obtain a good fit with experiment, at this energy, is a pronounced forward peak then our calculation fulfills that demand. However, this kind of statement must not be taken too seriously for two reasons: (1) our treatment

is, after all, an approximate one whereas CM's is exact and (2) we realize that this forward peak is not as stable as the rest of the curve with respect to variation of numerical parameters so that it has to be considered with some care.

We are aware that Liu [15] at IAMS performs new experiments for this system at this low-energy region. It will be interesting to see to what extent his new results will compare with the QM calculations.

3.2. Vibrational state-to-state integral cross-sections

In Fig. 3a are presented the individual integral cross-sections for each of the products. In Fig. 3b are

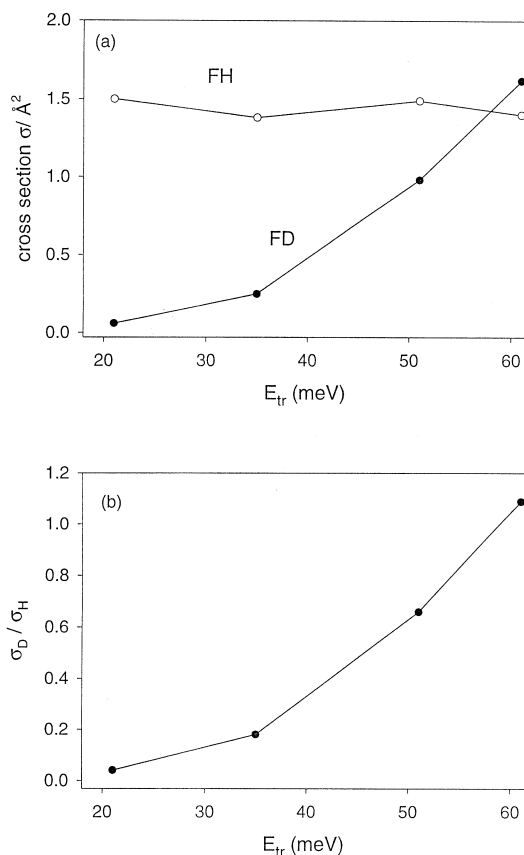


Fig. 3. (a) Total integral cross-sections σ_H and σ_D for the individual products as a function of energy. (b) Isotope effect I_{DH} ($= \sigma_D / \sigma_H$) as a function of energy.

presented the energy-dependent isotope effects I_{DH} defined as:

$$I_{\text{DH}} = \sigma_{\text{D}} / \sigma_{\text{H}}, \quad (5)$$

where σ_{H} and σ_{D} are the cross-section for reactions (Ia) and (Ib), respectively. The main features to be noticed are:

(1) Whereas the cross-section σ_{H} is only weakly dependent on the energy, the cross-section σ_{D} decreases rapidly as the energy approaches zero.

(2) The isotope effect, which in general in this energy range favors the formation of FH, is seen to increase rapidly with energy so that once the energy reaches the highest value it becomes somewhat larger than unity. In this respect it is interesting to note that the CM I_{DH} value is 0.96 for this energy, namely $\sim 10\%$ smaller.

The vibrational state-to-state and total integral cross-sections as a function of energy for reactions (Ia) and (Ib) are presented in Tables 1 and 2, respectively. The relative vibrational distributions are shown as well. In addition to the theoretical results, we present for each reaction Perry and Polanyi's (PP) [7] experimental vibrational distributions, as

Table 1

Vibrational state-to-state cross-sections (\AA^2) for the reaction $\text{F} + \text{HD} \rightarrow \text{FH} + \text{D}$ (numbers in parentheses are the relative values with respect to $v = 2$)

E_{total} (eV)	E_{tr} (meV)	$v = 0$	$v = 1$	$v = 2$	Total
0.254	21	0.02 (0.02)	0.09 (0.06)	1.39 (1.00)	1.50
0.268	35	0.01 (0.01)	0.06 (0.05)	1.31 (1.00)	1.38
0.284	51	0.02 (0.01)	0.11 (0.08)	1.36 (1.00)	1.49
0.294	61	0.04 (0.03)	0.17 (0.13)	1.34 (1.00)	1.55
0.294	61	0.01 ^a (0.01)	0.15 ^a (0.12)	1.24 ^a (1.00)	1.40 ^a
Exp-IR ^b		(0.03)	(0.29)	(1.00)	-

^aRef. [24].

^bRef. [7].

Table 2

Vibrational state-to-state cross-sections (\AA^2) for the reaction $\text{F} + \text{HD} \rightarrow \text{FD} + \text{H}$ (numbers in parentheses are the relative values with respect to $v = 3$)

E_{total} (eV)	E_{tr} (meV)	$v = 0$	$v = 1$	$v = 2$	$v = 3$	$v = 4$	Total
0.254	21	-	0.001 (0.03)	0.01 (0.35)	0.03 (1.00)	0.02 (0.67)	0.06
0.268	35	0.002 (0.01)	0.004 (0.03)	0.04 (0.29)	0.14 (1.00)	0.070 (0.50)	0.25
0.284	51	0.009 (0.02)	0.024 (0.04)	0.16 (0.30)	0.54 (1.00)	0.25 (0.46)	0.98
0.294	61	0.023 (0.02)	0.057 (0.06)	0.29 (0.32)	0.91 (1.00)	0.34 (0.37)	1.62
0.294	61	-	0.02 ^a (0.03)	0.20 ^a (0.31)	0.65 ^a (1.00)	0.47 ^a (0.72)	1.34 ^a
Exp-IR ^b		(0.07)	(0.15)	(0.50)	(1.00)	(0.55)	-

^aRef. [24].

^bRef. [7].

measured for a somewhat higher energy. The main features to be noticed are:

(1) The QM vibrational distributions are only weakly dependent on the energy. This is particularly interesting for the DF case because here the total cross-sections are strongly dependent on the energy.

(2) In all cases the FH vibrational distribution is sharply peaked at $v = 2$ whereas the FD distribution peaks at $v = 3$ (which, in contrast to the FH case, is not the highest vibrational state), but the distribution is much milder.

(3) The fit with PP's infrared chemiluminescence results (for our highest energy) is reasonable but not as well as could be expected recalling the good PES applied and the accuracy of the QM calculations. At this point we would like to mention that the $v = 3$ vibrational state, at this energy, which is open in the real FH molecule, is closed for the SW PES. This fact can have an effect on the QM calculations for this system but we do not think that the results are significantly affected by this defect.

(4) It is also interesting to note to what extent the CSA is capable of reproducing the exact results. In the case of FH the results are only a few percent apart, this applies also to the total cross-section. A

larger discrepancy is obtained for FD where the $v = 3$ is seen to be over populated at the expense of $v = 4$. Also, the total cross-sections in the case of FD are $\sim 20\%$ apart. The large discrepancy for this value is somewhat surprising because for $F + D_2$ at the energy of 90 meV the difference between the exact and the CSA cross-section was only 2–3%.

4. Conclusions

In this Letter a QM numerical study of reactions (Ia) and (Ib) at the low-energy region (near threshold, $21 \text{ meV} \leq E_{tr} \leq 61 \text{ meV}$) is presented. Two types of results were discussed:

(1) Vibrational state-to-state differential cross-sections were calculated for four energies, namely $E_{tr} = 21, 35, 51$ and 61 meV . The distributions for $E_{tr} = 61 \text{ meV}$ were compared with ‘exact’ results and the fit was found to be, qualitatively, acceptable. They show an ordinary backward distribution in the case of FD and a two-peak distribution (one forward and one backward) for FH. Similar distributions (not presented) were obtained for $E_{tr} = 51 \text{ meV}$. The distributions at $E_{tr} = 35 \text{ meV}$ are as follows: in the case of FD the distribution is as before, namely backward peaked, but in the case of FH a change occurs, namely in addition to the backward and the forward peaks a third peak appears at $\theta \approx 110^\circ$. This phenomenon is attributed to the strong tunneling process that takes place at this energy region and the existence of shallow potential wells which are capable of forming bound states, thus leading to the build-up of resonances. At $E_{tr} = 21 \text{ meV}$ (not shown here) we got pure backward distributions for both DF and HF.

(2) A very strong isotope effect was revealed at this energy interval. We found that I_{DH} (defined in Eq. (5)) changes from 0.04 at $E_{tr} = 21 \text{ meV}$ to ~ 1.0 at $E_{tr} = 61 \text{ meV}$. This effect is attributed to the selection capability of the (dynamic) barrier in the entrance channel. It enables the hydrogen atom to tunnel through almost freely but at the same time severely limits the passage of deuterium.

Acknowledgements

I would like to thank Professors Y.T. Lee and S.H. Lin for their warm hospitality at the IAMS,

Professor K. Liu for many lively discussions on this subject and the Academia Sinica for supporting this research.

References

- [1] R.D. Levine, R.B. Bernstein, *Molecular Reaction Dynamics and Chemical Reactivity*, Oxford University Press, Oxford, 1987.
- [2] T.P. Shafer, P.E. Siska, J.M. Marson, F.P. Tully, Y.C. Wong, Y.T. Lee, *J. Chem. Phys.* 53 (1970) 3385.
- [3] D.M. Neumark, A.M. Wodtke, G.N. Robinson, C.C. Hayden, Y.T. Lee, *J. Chem. Phys.* 82 (1985) 3045.
- [4] D.M. Neumark, A.M. Wodtke, G.N. Robinson, C.C. Hayden, K. Shobatake, R.K. Sparks, Y.P. Shafer, Y.T. Lee, *J. Chem. Phys.* 82 (1985) 3067.
- [5] J.C. Polanyi, S. Woodall, *J. Chem. Phys.* 57 (1972) 1575.
- [6] J.C. Polanyi, J.L. Schriber, *Faraday Discuss., Chem. Soc.* 62 (1977) 267.
- [7] D.S. Perry, J.C. Polanyi, *Chem. Phys.* 12 (1977) 37.
- [8] M. Faubel, L.Y. Rusin, S. Schlemmer, S. Somdrman, U. Tapp, J.P. Toennies, *J. Chem. Phys.* 101 (1994) 2106.
- [9] M. Faubel, B. Martin'ez-Haya, L.Y. Rusin, U. Tapp, J.P. Toennies, F.J. Aoiz, L. Banares, *J. Phys. Chem. A* 102 (1998) 8695.
- [10] M. Baer, M. Faubel, B. Martinez-Haya, L.Y. Rusin, U. Tapp, J.P. Toennies, K. Stark, H.-J. Werner, *J. Chem. Phys.* 104 (1996) 2743.
- [11] M. Baer, M. Faubel, B. Martin'ez-Haya, L.Y. Rusin, U. Tapp, J.P. Toennies, *J. Chem. Phys.* 108 (1998) 9694.
- [12] G. Dharmasena, K. Kopeland, J.H. Young, R.A. Lassel, T.R. Philips, K. Shokhirev, G.A. Parker, M. Keil, *J. Phys. Chem.* 101 (1997) 6429.
- [13] W.B. Chapman, B.W. Blackman, S. Nizkorodov, D.J. Nesbitt, *J. Chem. Phys.* 109 (1998) 9306.
- [14] M. Baer, M. Faubel, B. Martinez-Haya, L.Y. Rusin, U. Tapp, J.P. Toennies, *J. Chem. Phys.* 110 (1999) 10231.
- [15] K. Liu, private communication.
- [16] S.F. Wu, B.R. Johnson, R.D. Levine, *Mol. Phys.* 25 (1973) 839.
- [17] G.C. Schatz, J.M. Bowman, A. Kuppermann, *J. Chem. Phys.* 56 (1973) 4023.
- [18] J. Jellinek, M. Baer, D.J. Kouri, *Phys. Rev. Lett.* 47 (1981) 1588.
- [19] V. Khare, D.J. Kouri, M. Baer, *J. Chem. Phys.* 71 (1979) 1188.
- [20] J.T. Muckerman, *J. Chem. Phys.* 56 (1972) 2997.
- [21] T. Takayanagi, S. Tsunashima, S. Sato, *J. Chem. Phys.* 93 (1990) 2487.
- [22] K. Stark, H.-J. Werner, *J. Chem. Phys.* 104 (1996) 6515.
- [23] J.F. Castillo, D.E. Manolopoulos, K. Stark, H.-J. Werner, *Chem. Phys.* 104 (1996) 6531.
- [24] J.F. Castillo, D.E. Manolopoulos, *Faraday Discuss., Chem. Soc.* 110 (1998) 119.
- [25] P. Honvault, J.M. Launay, *Chem. Phys. Lett.* 303 (1999) 657.

- [26] E. Rosenman, Z. Hochman-Kowal, A. Persky, M. Baer, *Chem. Phys. Lett.* 257 (1996) 421.
- [27] H. Wang, W.H. Thompson, W.H. Miller, *J. Phys. Chem.* 102 (1999) 9372.
- [28] A. Persky, *J. Chem. Phys.* 59 (1973) 3612.
- [29] A. Persky, *J. Chem. Phys.* 59 (1973) 5578.
- [30] M. Baer, D. Neuhauser, Y. Oreg, *J. Chem. Soc., Faraday Trans.* 86 (1990) 1721.
- [31] M. Baer, H. Nakamura, *J. Chem. Phys.* 96 (1992) 6565.
- [32] I. Last, A. Baram, H. Szichman, M. Baer, *J. Phys. Chem.* 97 (1993) 7040.
- [33] I. Last, M. Baer, in: J.M. Bowman (Ed.), *Advances in Molecular Vibrations and Collision Dynamics*, vol. 2A, JAI Press, Greenwich, CT, 1994, p. 85.
- [34] M. Baer, I. Last, H.-J. Loesch, *Chem. Phys.* 101 (1994) 9648.
- [35] D. Neuhauser, M. Baer, *J. Chem. Phys.* 90 (1989) 4351.
- [36] P. McGuire, D.J. Kouri, *J. Chem. Phys.* 60 (1974) 633.